

Effect of Different Heat Treatments on Microstructure and Mechanical Properties of Ti6Al4V Titanium Alloy

Liu Wanying^{1,2}, Lin Yuanhua^{2,3}, Chen Yuhai², Shi Taihe³, Ambrish Singh^{2,4}

¹ Sichuan University, Chengdu 610065, China; ² School of Materials Science and Engineering, Southwest Petroleum University, Chengdu 610500, China; ³ State Key Laboratory of Oil and Gas Reservoir Geology and Exploitation, Southwest Petroleum University, Chengdu 610500, China; ⁴ Lovely Faculty of Technology and Sciences, Lovely Professional University, Phagwara, Punjab, India

Abstract: This paper analyzed the microstructure of Ti6Al4V titanium alloy after different heat treatments. The tensile experiment and instrumented impact test were performed. The relationship among the microstructure, impact fracture characteristic and mechanical properties was analyzed by metallurgical microscope and environment scanning electron microscope (ESEM). Results show that the microstructure, mechanical properties and impact toughness of Ti6Al4V titanium alloy are affected by the solution and aging treatment. The yield strength and ultimate tensile strength are improved remarkably. The ductility increases firstly, and then decrease. The good comprehensive properties can be obtained when the Ti6Al4V titanium alloy is treated under the condition of 960 °C/1 h + WQ and 500 °C/4 h + AC. $\sigma_{0.2}$ is 1050 MPa, σ_b is 1120 MPa and A_k is 46.22 J cm⁻². The microstructure of the titanium alloy after solution and aging treatment consists of the β matrix and the precipitation of the α -phase. The lamellar β -phase and the α -phase structure of the small needle plexiform can enhance comprehensive properties.

Key words: heat treatment; Ti6Al4V titanium alloy; microstructure; mechanical property

Titanium and its alloys are ideal materials for aerospace industry because of the high strength^[1] to resist high temperature. Moreover they are ideal materials for marine, petroleum, chemical, pharmaceutical and other industries due to good corrosion resistance^[2-5]. With the rapid development of modern oil industry, oil and gas drilling puts forward higher requirements for the drilling technology, especially some particular processes of well drilling. Some conventional drilling tools are unable to meet drilling requirements. A series of drilling tools are developed for meeting requirements of special and complex wells^[6]. Titanium alloy drill pipe is a new variety of recently developed products. It has less structural stress, good flexibility, fatigue resistance, corrosion resistance and light mass comparing to conventional steel drill pipe. Furthermore it has good adaptability in the high curvature borehole drilling applications^[7-10]. Ti6Al4V alloy has high tensile strength and resistance fatigue strength, low modulus

of elasticity, low density, high hardness and good corrosion resistance. It's often used as the drill pipe. The Grant Prideco subsidiary of Weatherford and RTI International company in the Texas subsidiary RTI Energy Systems has developed a titanium alloy drill pipe, which not only has the strength of steel drill pipe, but also is a flexible and light, synthetic material with corrosion resistance and durability^[11-14]. However, the toughness of Ti6Al4V alloy is poor, which restricts its wide application and promotion in oil field. Material's properties are determined by the microstructure. Titanium alloy's microstructure can't be altered or controlled by varieties of thermo-mechanical treatments^[15,16]. Heat treatment can improve its microstructure and mechanical properties. Some studies show rapid heat treatment can provide a significant improvement of intragrain structure and mechanical properties of cast ($\alpha+\beta$)-titanium alloys. Once a paper reported the Ti6Al4V alloy with a coarse grain α -phase

Received date: March 10, 2016

Foundation item: National Natural Science Foundation of China (51274170); Open Fund Project (x151514kcl108); College Students Innovative and Entrepreneurial Training Program (201410615022)

Corresponding authors: Liu Wanying, Ph. D., Lecturer, School of Materials Science and Engineering, Southwest Petroleum University, Chengdu 610500, P. R. China, Tel: 0086-28-83037431, E-mail: liuwanyingxx@163.com

Copyright © 2017, Northwest Institute for Nonferrous Metal Research. Published by Elsevier BV. All rights reserved.

preform condition required longer heat treatment time to refine the structure and provided a modest improvement in mechanical properties^[17,18]. Some studies about curves of grain size of primary α -phase are oscillatory in the $\alpha+\beta$ two-phase region with the rise of deformation temperature. Meanwhile the volume fraction of primary α -phase decreases. Heat treatment has a very important role in affecting microstructure and improving comprehensive properties of titanium alloy^[19-21]. The purpose the present paper is to explore parameters for improving microstructure and mechanical properties of Ti6Al4V alloy through different solution and aging treatments.

1 Experiment

The test material is a hot-rolled Ti6Al4V titanium alloy with high strength and its thickness is 6 mm. Its chemical compositions (mass fraction, %) are iron (Fe)<0.25, carbon (C)<0.06, hydrogen (H)<0.008, nitrogen (N)<0.040, oxygen (O)<0.065, aluminum (Al) 5.5~6.2, vanadium (V) 3.5~4.0 and the balance is Ti.

Six preliminary heat treatment systems were selected in the experiment. It is decided according to the temperature of phase transition. The heat treatment processes are shown in Table 1. The Ti6Al4V alloy was heat treated before the fracture toughness test for determine the influence of ($\alpha+\beta$)-phase morphology on its fracture toughness. Heat treatment was conducted in the SX-4-13 box-type resistance furnace. When the heat treatment finished, the microstructure analysis, tensile mechanical test, instrument impact test, X-ray diffraction (XRD) test and environment scanning electron microscope (ESEM) observation of fracture morphology were carried out.

The Ti6Al4V alloy tube before and after heat treatment was processed into lath tensile specimens. A static tensile test was carried out on the MTS810 hydraulic servo universal testing machine. The dimension of parameters which tensile specimens include is described as follows. The thickness is 7 mm. The width is (20±0.05) mm. The gauge length is (60+0.5) mm. The length of clamping end is 50 mm. The curvature length between parallel segment and clamping end is greater than or equal to 12. The total length of tensile sample is greater than or

equal to 184 mm. The strain rate was $\dot{\epsilon} = 0.003 \text{ s}^{-1}$. The tensile test conformed to ISO 6892:1998. The tensile strength σ_b and yield strength $\sigma_{0.2}$ and elongation δ were measured.

The fracture toughness was tested through an instrumented impact test according to the standard of Metal Charpy Notched Impact Test Method. The dimension of specimens is 10 mm×5 mm×55 mm. The equipment is an impact testing machine of ZBC2302-D type. Its impact energy is 294 J and the impact rate is 5.24 m/s.

The microstructure of specimens before and after heat treatment was analyzed by an Olympus PMG-type 3 microscope. Specimens were round, polished and etched at 270 K in a reagent which is 1 mL HF+30 mL HNO₃+30 mL H₂O₂. The impact fracture was observed by the FEI Quanta 450 ESEM. Fractographic observation was indispensable in analyzing fracture feature and mechanism.

2 Results and Discussion

The α -phase is the substrate phase of ($\alpha+\beta$)-titanium alloy. The number, shape and size of α -phase determine directly the property of ($\alpha+\beta$)-titanium alloy. In the two-phase region, ($\alpha+\beta$)-phase is gotten from the heat treatment with different holding time and temperatures. The temperature is below the phase transition temperature. The main characteristics of ($\alpha+\beta$)-phase microstructure are irregular shape of grains, continuous and discontinuous α -phase on the grain boundary, and many small secondary α -phases. The punctate, spherical, flakiness and short rod α -phase exists in intragranular^[22]. However, all ($\alpha+\beta$)-phase will be converted into β -phase when the heating temperature is higher than phase transition temperature. The size and shape of grains are not identical. They are quadrilateral, pentagon and hexagon.

Solution and aging can eliminate or reduce α -phase of continuous grain boundary. They can improve significantly the tensile and fatigue strength. But the plasticity will decrease a little. Solution and aging treatment can improve obviously the fatigue strength. The more stable β -phase of alloy, the more β -phase metastable after quenching. Then the effect of aging strengthening is better. Maximum effect will be gotten when the temperature of β stable element reaches C_K value. Strengthening effect decreases with the rise of β -phase. That causes precipitation of aging β -phase metastable and the number of α -phase declines. Ti6Al4V alloy is ($\alpha+\beta$)-phase alloy. The microstructure and mechanical properties can be improved by the solution and aging heat treatment, and then better comprehensive properties can be obtained^[23,24].

2.1 Influence of heat treatment on microstructure of Ti6Al4V Alloy

Microstructures of Ti6Al4V alloy after different heat treatments can be seen in Fig.1. According to the microstructure obtained, the heating temperature is under ($\alpha+\beta$)→ β transus temperature, and much equiaxed structure can be

Table 1 Heat treatment process of Ti6Al4V alloy

| Solution temperature/ °C | Insulation time/h | Cooling method | Aging temperature/ °C | Insulation time/h | Cooling method |
|-----------------------------|-------------------|----------------|--------------------------|-------------------|----------------|
| 920 | 1 | WQ | 450 | 4 | AC |
| 920 | 1 | WQ | 500 | 4 | AC |
| 960 | 1 | WQ | 450 | 4 | AC |
| 960 | 1 | WQ | 500 | 4 | AC |
| 1000 | 1 | WQ | 450 | 4 | AC |
| 1000 | 1 | WQ | 500 | 4 | AC |

Note: WQ is water quenching and AC is air cooling

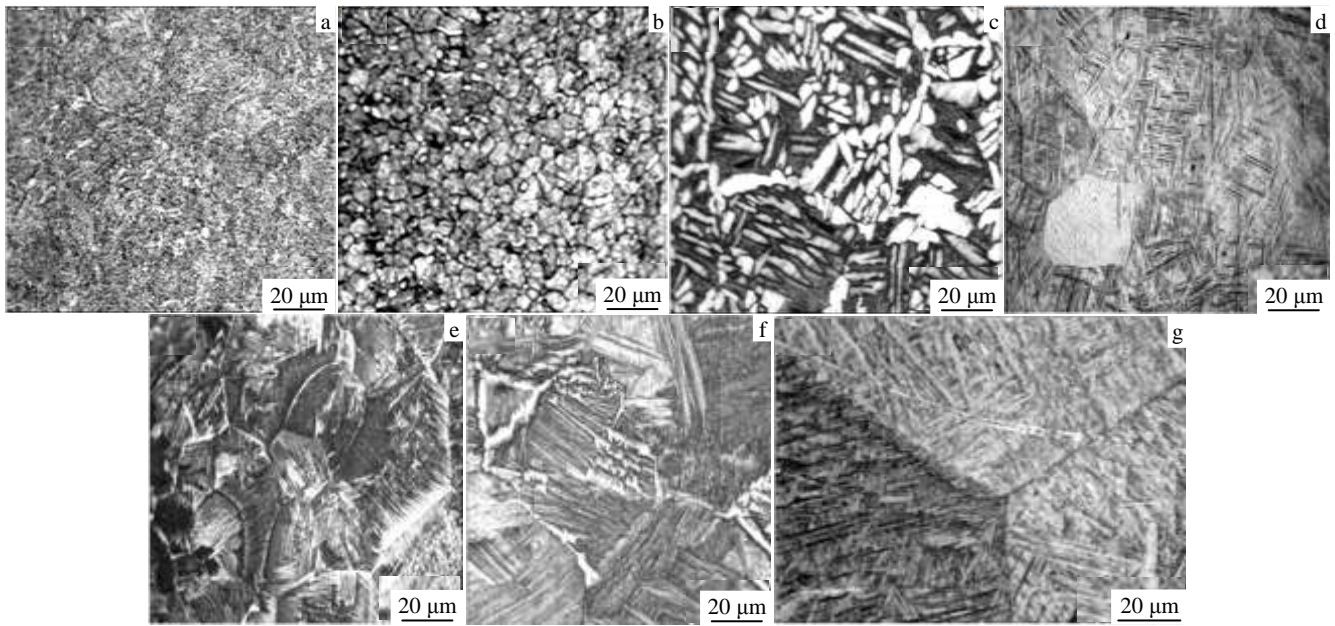


Fig.1 Microstructures of Ti6Al4V alloy under different heat treatment conditions: (a) hot-rolled (no heating); (b) 920 °C/1 h + WQ, 450 °C/4 h+AC; (c) 920 °C/1 h+WQ, 500 °C/4 h+AC; (d) 960 °C/1 h+WQ, 450 °C/4 h+AC; (e) 960 °C/1 h+WQ, 500 °C/4 h +AC; (f) 1000 °C/1 h+WQ, 450 °C/4 h+AC; (g) 1000 °C/1 h+WQ, 500 °C/4 h+AC

obtained. But the proportion of shifting organization is less. When the heating temperature is higher than the $(\alpha+\beta)\rightarrow\beta$ transus temperature, the coarse grains and sheet microstructure can be obtained. It can be seen clearly that original β grain and obvious α -phase appear separately along the grain boundary. The original β grain transforms to the long and staggered microstructure, which braids in different places. Fig.1a is the microstructure of annealed alloy. It is a mixture of the primary α -phase and $(\alpha+\beta)$ -phase. From Fig.1b to Fig.1f, it can be seen that the microstructure consists of β -phase and $(\alpha+\beta)$ -phase when the alloy is treated by solution and aging. But the microstructure after aging is coarser. The quenching temperature of Fig.1b is 920 °C and α' -phase is fewer and smaller after quenching. The α' -phase converts into the mixture of fine and lamellar $(\alpha+\beta)$ -phase after aging treatment. The size of α' -phase becomes larger with the rise of aging temperature. The α' -phase with large size will convert to large $(\alpha+\beta)$ -phase with larger lamellar spacing after heat treatment. It can be seen from Fig.1c. That is a typical two-state microstructure. It can be gotten when the temperature is lower than the transus temperature. Comparing to α -phase of the solid solution, the size of α' -phase after aging gets coarser obviously. It can be speculated that α -phase which precipitates from α' -phase does not only forming lamellar, but also grows along the primary α -phase. So the size of α -phase gets coarser finally. The full solubility of strengthening phase and the uniform distribution of alloy elements on the grain boundary with the rise of solution temperature are presented in Fig.1d. With the rise of aging

temperature, $(\alpha+\beta)$ -phase crystal grain increases gradually and gets bigger. At the same time, β -phase recrystallizes. Because β -phase increases, the diffusion of atom, the dissolution of phase, precipitation and gathering in the process of phase transition, leads β -phase to distribute in the islet near α crystal grain. When the temperature approaches to the β transus temperature, β -phase becomes the basal body. This microstructure has good plasticity and stability, but the creep property is poor. Martensite converts into α' -phase and metastable β -phase during the quenching course. It can be seen that the primary α -phase transforms completely into β -phase from Fig.1e. The lamellar β -phase and survival α -phase are arranged in the shape of group beam. The α -phase not only distributes uniformly along the grain boundary, but also arranges parallelly in the form of bundles which is embedded in β crystalline grain. Hence an obvious basket-like microstructure is obtained. The crystalline grain gets smaller, so comprehensive properties are improved. Because the cooling is water, β -phase in the high temperature section from the process of rapid cooling is too late to convert to α -phase. The martensite α'' and metastable state β -phase are gotten. The α'' and metastable state β -phase begin to decompose and produce dispersive $(\alpha+\beta)$ -phase basket-like microstructure with good fatigue property and other comprehensive properties. The dimension of schistose β -phase gets smaller and stagger mutually. The microstructure is fined. That improves comprehensive properties of the alloy. From Fig.1e, the crystal grains become coarse and their size gets large with the solution temperature increasing. Moreover

it is the shape of flaky microstructure and obvious α -phase appears. The α -phase with layered arrangement is embedded in the β -phase. Some residual α -phase distributes unevenly along the crystalline grain staggered microstructure like long strip. From Fig.1g, crystalline grains like lamellar are coarse. Original β crystalline grains convert into staggered microstructure like long strip.

2.2 Influence of heat treatment on tensile properties of Ti6Al4V alloy

Table 2 shows the influence of solution and aging treatment on mechanical properties of Ti6Al4V alloy. The strength of Ti6Al4V alloy is improved greatly when the hot rolled state alloy experiences solution and aging treatment. The elongation is somewhat increased except for individual process. No.5 process can obtain the best comprehensive property with the parameters of 960 °C/1 h+WQ and 500 °C/4 h+AC. Comparing with that of the hot-rolled, yield strength ($\sigma_{0.2}$) is increased by 50%, ultimate tensile strength (σ_b) by 42% and elongation δ increase by 11%. The strength and elongation increase with the rise of quenching temperature. But they increased firstly and then decrease. It could be presented the best solution temperature is 960 °C and the best aging temperature is 500 °C. When the Ti6Al4V alloy is heat treated by aging temperature 500 °C, the basket-like microstructure β -phase and ($\alpha+\beta$)-phase mixture are obtained just like Fig.1e. They distribute near the crystalline boundary inside the α crystalline grain. That will make the alloy have good strength and elongation. It is noted that the strength of Ti6Al4V alloy increases when the solid-solution β -phase converts into martensite (α' -phase). Then martensite (α' -phase) converts into fine α -phase and β -phase. According to the description mentioned above, α -phase declines and β -phase increases in number. More α' -phase are converted from β -phase with the gradual rise of quenching temperature. Obviously, the more α' -phase, the better strength is gotten. The excessive coarse α -phase is preserved when solution temperature is too high. That results in the uneven material microstructure and thus the strength is possible to decrease due to stress concentration.

Table 2 Heat treatment processes and mechanical properties

| Heat treatment processes | $\sigma_{0.2}/\text{MPa}$ | σ_b/MPa | $\delta/\%$ |
|-------------------------------------|---------------------------|-----------------------|-------------|
| Hot rolled | 700 | 790 | 12.81 |
| 920 °C/1 h + WQ 450 °C/4 h + AC | 890 | 1000 | 15.00 |
| 920 °C/1 h + WQ 500 °C/4 h + AC | 960 | 1070 | 13.82 |
| 960 °C/1 h + WQ 450 °C/4 h + AC | 960 | 1050 | 15.48 |
| 960 °C/1 h + WQ 500 °C/4 h + AC | 1050 | 1120 | 16.28 |
| 1000 °C/1 h + WQ 450 °C/4 h + AC | 1000 | 1100 | 12.08 |
| 1000 °C/1 h + WQ 500 °C/4 h + AC | 1020 | 1100 | 10.23 |

2.3 Instrumented impact fracture toughness

2.3.1 Influence of heat treatment on impact toughness

Table 3 shows the impact toughness of samples. The result is compared with the hot rolled sample's impact toughness. It can be seen that the impact toughness value decreases with the rise of solution temperature. The impact toughness in aging temperature 450 °C is stabler than that at 500 °C. The best impact toughness is obtained when solution temperature is 960 °C, because when the quenching temperature is higher the α -phase microstructure is coarser. It will decrease the plasticity and toughness. The material toughness decreases with the rise of aging temperature when solution temperature is 920 °C. The toughness A_k is 40 J cm⁻² when the aging temperature is 450 °C; the toughness A_k is 38.21 J cm⁻² when aging temperature is 500 °C. With the rise of solution temperature, the curve of their correlation under certain aging temperature condition is shown in Fig.3. The toughness increases with the decrease of aging temperature when solution temperature is 1000 °C. The toughness A_k is 30.63 J cm⁻² when aging temperature is 500 °C; the toughness A_k is 33.05 J cm⁻² when aging temperature is 450 °C.

2.3.2 ESEM analysis of the impact fracture

For analyzing the relationship between plastic fracture characteristics and microstructure of the material after heat treatment, the ESEM analysis of impact fracture from process 3 to 6 was carried out in order to determine the plasticity of the material under different conditions. The results are shown in Fig.2. Dimples are deep and big in Fig.2a. Its plasticity and toughness are good. It can be seen clearly the fracture forms along the crystalline grain. The less toughness fracture characteristic is seen from Fig.2b. The layer fracture along the direction of the lamellar structure phase can be seen in Fig.2c. The ability of thick slices of layered microstructure on the material resisting the fatigue cracking gets lower. The dimple is deep and big in Fig.2d and distributes evenly. It is obvious ductile fracture. The β metastable phase decomposes after solution and aging treatment. The α -phase precipitates preferentially and it distributes uniformly in crystalline grain boundary and β -phase. Finally ($\alpha+\beta$)-phase is combined, which improves the strength and toughness obviously and enhances comprehensive properties. Dimples of Fig.2e are shallow that lead to the poor plastic and toughness. With the solution temperature increases and the aging temperature

Table 3 Heat treatment processes and impact toughness

| Heat treatment processes | Impact energy, $A_k/\text{J cm}^{-2}$ |
|--------------------------------|---------------------------------------|
| Hot rolled (no heat treatment) | 27.60 |
| 920 °C/1 h+WQ, 450 °C/4 h+AC | 40.00 |
| 920 °C/1 h+WQ, 500 °C/4 h+AC | 38.21 |
| 960 °C/1 h+WQ, 450 °C/4 h+AC | 43.64 |
| 960 °C/1h+WQ, 500 °C/4 h+AC | 46.22 |
| 1000 °C/1 h+WQ, 450 °C/4 h+AC | 33.05 |
| 1000 °C/1 h+WQ, 500 °C/4 h+AC | 30.63 |

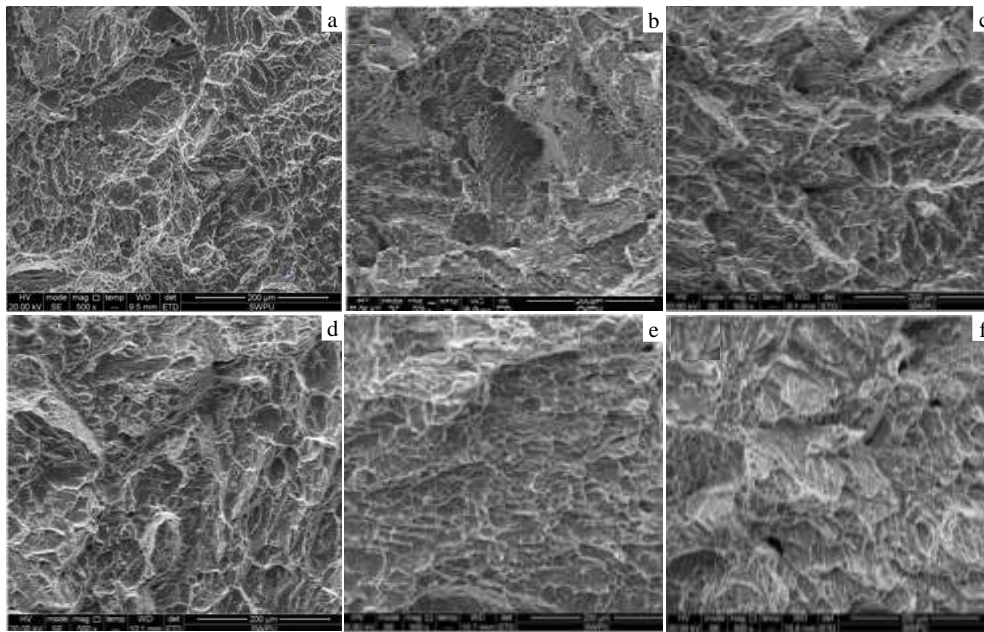


Fig.2 ESEM micrographs of impact fracture morphologies: (a) 920 °C/ 1 h + WQ, 450 °C/4 h + AC; (b) 920 °C/1 h + WQ, 500 °C/4 h + AC; (c) 960 °C/1 h + WQ, 450 °C/4 h + AC; (d) 960 °C/1 h + WQ, 500 °C/4 h + AC; (e) 1000 °C/1 h + WQ, 450 °C/4 h + AC; (f) 1000 °C/1 h + WQ, 500 °C/4 h + AC

decreasing, a large number of β metastable phase form with uneven distribution of α -phase in the crystalline grain boundary and territory. The fracture characteristic declines to quasi-cleavage fracture in the Fig.2f. It is noted that the fracture is prone to brittle fracture. Based on the two-phase titanium alloy, Ti6Al4V titanium alloy has the small, uniform spherical and basket-like mixture microstructure β -phase and ($\alpha+\beta$)-phase. In the process of instrumented impact fracture experiment, the hole will form in the original phase and the boundary of the conversation microstructure. With the rise of impact deformation degree, these holes get bigger along the boundary of phase before the β -phase is across the cluster. The microstructure of mixture phase grows up comparing to the hole. The crack extension has the blocking effect. Therefore the mechanical property is affected by its shape, distribution, dimension and so on. It is concluded that two-state microstructure of two-phase is effective to block cavity growing and cracks extension.

3 Conclusions

1) The better microstructure of Ti6Al4V titanium alloy can be obtained in the process of 960 °C/1 h + WQ and 500 °C/4 h + AC, which is basket weave microstructure of lamellar β -phase and residual α -phase. It can produce good comprehensive properties.

2) Ti6Al4V alloy's strength increases with the rise of solution temperature, and then it decreases. But ductility and impact toughness decreases gradually. However the strength decreases, but ductility and impact toughness increases firstly,

and then decreases with the rise of aging temperature.

3) The fracture characteristic is transgranular ductile fracture. The α -phase distributes unevenly that reduces the plastic and the toughness.

References

- Li G Y, Jiang Y R, Huang K L et al. *Journal of Alloys And Compounds*[J], 2008, 466(1): 456
- Zhang Q L, Kuang Y R, Han Y B et al. *The Chinese Journal of Nonferrous Metals*[J], 2012, 22(10): 2756 (in Chinese)
- Kung K C, Yuan K, Li T M et al. *Journal of Alloys And Compounds*[J], 2012, 515: 68
- Peng Y P, Zeng F C, Wang J J et al. *Journal of Materials Engineering*[J], 1997(10): 3 (in Chinese)
- Gu X Z, Li G, Chai P. *The Seventh International Symposium of Friction Stir Welding*[R]. Cambridge: Welding Institute, 2008
- Luzhnikov L P, Novikova V M, Mareev V M. *Metallovedenie Termicheskaya Obrabotka Metallov*[J], 1965, 7(5): 56
- Luo J, Li M Q, Yu W X. *Rare Metal Materials and Engineering*[J], 2010, 39(8): 1323 (in Chinese)
- Kolachev B A, Mamonova F S. *Metallovedenie Termicheskaya Obrabotka Metallov*[J], 1975, 17(8): 52
- Yuan W Y, Zhang Q H. *Xinjiang Petroleum Technology*[J], 2006 (3): 13 (in Chinese)
- Lei W G, Mao X N, Lu Y F. *Heat Treatment of Metals*[J], 2012, 37(9): 110 (in Chinese)
- Shi X L, Wang Q L, Wang F C et al. *Journal of Materials Science & Technology*[J], 2009, 19(2): 220
- Xiong A M, Huang W C, Chen S H et al. *The Chinese Journal of*

- Nonferrous Metals*[J], 2002, 12(s1): 206 (in Chinese)
- 13 Wang X Y, Xie C M. *Special Casting & Nonferrous Alloys*[J], 2001(6): 16 (in Chinese)
- 14 Huang X, Cuddy J, Goel N et al. *Journal of Materials Engineering and Performance*[J], 1994, 3(4): 560
- 15 Gu X H, Liu J, Shi J H. *Heat Treatment of Metals*[J], 2011, 36(2): 29 (in Chinese)
- 16 Yang H Y, Chen J, Zhao Y Q. *Development and Application of Materials*[J], 2009, 24(2): 13 (in Chinese)
- 17 Markovskya P E, Semiatiin S L. *Journal of Materials Science and Engineering*[J], 2011, 2(1): 3079
- 18 Cai J, Li F G, Liu T Y et al. *Materials Characterization*[J], 2011, 62(3): 287
- 19 Wang Q, Li Z H, Sun D L. *Key Engineering Materials*[J], 2005, 297: 1439
- 20 Chen Y H, Wang S Y, Sun X et al. *New Technology & New Proces*[J], 2009 (12): 124
- 21 Guo P, Gong Q, Qi Y L. *New Technology & New Proces*[J], 2010, 27: 22
- 22 He H B, Zhou W L, Chen G Q et al. *Materials For Mechanical Engineering*[J], 2009, 33: 79
- 23 Du S M, Pan C H. *Transactions of Materials and Heat Treatment* [J], 2009, 18: 113
- 24 Moskalewicz T, Wendler B, Zimowski S et al. *Surface & Coatings Technology*[J], 2010, 105: 2668

不同热处理工艺对 Ti6Al4V 钛合金微观结构和力学性能影响

刘婉颖^{1,2}, 林元华^{2,3}, 陈宇海², 施太和³, Ambrish Singh^{2,4}

(1. 四川大学, 四川 成都 610065)

(2. 西南石油大学 材料科学与工程学院, 四川 成都 610500)

(3. 西南石油大学 油气藏地质及开发工程国家重点实验室, 四川 成都 610500)

(4. Lovely Faculty of Technology and Sciences, Lovely Professional University, Phagwara, Punjab, India)

摘要: 通过对 Ti6Al4V 钛合金进行不同工艺的热处理, 分析了不同工艺处理后的显微组织, 进行了拉伸试验、示波冲击试验测试。研究固溶时效处理对 Ti6Al4V 钛合金显微组织、力学性能和冲击韧性的影响。利用金相显微镜、环境扫描电镜 (ESEM) 进一步分析了钛合金的组织、冲击断口特征与力学性能间的关系。结果表明, 随固溶温度升高, 钛合金屈服强度和抗拉强度得到显著提高, 塑韧性先增加后降低。优化热处理工艺后, Ti6Al4V 钛合金经 960 °C/1 h + WQ 和 500 °C/4 h + AC 处理, 获得优良综合性能, $\sigma_{0.2}$ 为 1050 MPa, σ_b 为 1120 MPa, A_k 为 46.22 J cm⁻²。钛合金固溶时效后的组织由 β 基体和析出的 α 相组成, 片层状 β 相和小针丛状 α 相组织能提高合金综合性能。

关键词: 热处理; Ti6Al4V 钛合金; 微观结构; 力学性能

作者简介: 刘婉颖, 女, 1983 年生, 博士, 讲师, 西南石油大学材料科学与工程学院, 四川 成都 610500, 电话: 028-83037431, E-mail: liuwanyingxx@163.com